

PROOF COVER SHEET

Author(s):	Rodolfo O. Esquivel
Article title:	Information-theoretical complexity for the hydrogenic abstraction reaction
Article no:	TMPH-607780
Enclosures:	1) Query sheet 2) Article proofs

Dear Author,

1. Please check these proofs carefully. It is the responsibility of the corresponding author to check these and approve or amend them. A second proof is not normally provided. Taylor & Francis cannot be held responsible for uncorrected errors, even if introduced during the production process. Once your corrections have been added to the article, it will be considered ready for publication.

For detailed guidance on how to check your proofs, please see <http://journalauthors.tandf.co.uk/production/checkingproofs.asp>.

2. Please review the table of contributors below and confirm that the first and last names are structured correctly and that the authors are listed in the correct order of contribution. This check is to ensure that your name will appear correctly online and when the article is indexed.

Sequence	Prefix	Given name(s)	Surname	Suffix
1		Rodolfo O.	Esquivel	
2		Moyocoyani Molina-	Espiritu	
3		Juan Carlos	Angulo	
4		Juan	Antolin	
5		Nelson Flores-	Gallegos	
6		Jesus S.	Dehesa	

Queries are marked in the margins of the proofs. Unless advised otherwise, submit all corrections and answers to the queries using the CATS online correction form, and then press the “Submit All Corrections” button.

AUTHOR QUERIES

General query: You have warranted that you have secured the necessary written permission from the appropriate copyright owner for the reproduction of any text, illustration, or other material in your article. (Please see <http://journalauthors.tandf.co.uk/preparation/permission.asp>.) Please check that any required acknowledgements have been included to reflect this.

AQ1	Ref [15] – provide year.

How to make corrections to your proofs using Adobe Acrobat

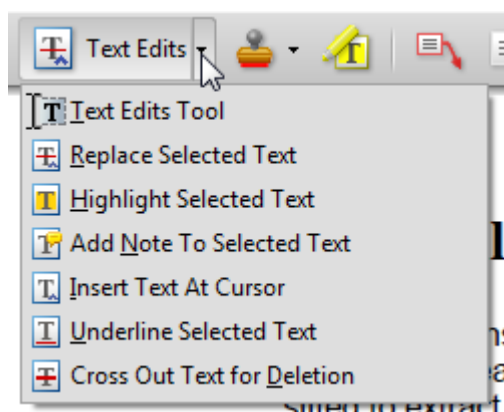
Taylor & Francis now offer you a choice of options to help you make corrections to your proofs. Your PDF proof file has been enabled so that you can edit the proof directly. This is the simplest and best way for you to ensure that your corrections will be incorporated. To do this, please follow these instructions:

1. Check which version of Adobe Acrobat you have on your computer. You can do this by clicking on the “Help” tab, and then “About”.

If Adobe Reader is not installed, you can get the latest version free from <http://get.adobe.com/reader/>.

- If you have Adobe Reader 8 (or a later version), go to “Tools”/ “Comments & Markup”/ “Show Comments & Markup”.
- If you have Acrobat Professional 7, go to “Tools”/ “Commenting”/ “Show Commenting Toolbar”.

2. Click “Text Edits”. You can then select any text and delete it, replace it, or insert new text as you need to. It is also possible to highlight text and add a note or comment.



3. Make sure that you save the file when you close the document before uploading it to CATS. A full list of the comments and edits you have made can be viewed by clicking on the “Comments” tab in the bottom left-hand corner of the PDF.

If you prefer, you can make your corrections using the CATS online correction form.

Information-theoretical complexity for the hydrogenic abstraction reaction

Rodolfo O. Esquivel^{abc*}, Moyocoyani Molina-Espíritu^a, Juan Carlos Angulo^{bc}, Juan Antolín^{cd},
Nelson Flores-Gallegos^c and Jesús S. Dehesa^{bc}

^aDepartamento de Química, Universidad Autónoma Metropolitana-Iztapalapa, 09340-México D.F., México; ^bDepartamento de Física Atómica, Molecular y Nuclear, Universidad de Granada, 18071-Granada, Spain; ^cInstituto Carlos I de Física Teórica y Computacional, Universidad de Granada, 18071-Granada, Spain; ^dDepartamento de Física Aplicada, EUITIZ, Universidad de Zaragoza, 50018-Zaragoza, Spain; ^eUnidad Profesional Interdisciplinaria de Ingeniería, Campus, Guanajuato del Instituto Politécnico Nacional, 36275-Guanajuato, México

(Received 4 April 2011; final version received 26 May 2011)

In this work, we have investigated the complexity of the hydrogenic abstraction reaction by means of information functionals such as disequilibrium (D), exponential entropy (L), Fisher information (I), power entropy (J) and joint information-theoretic measures, i.e. the I - D , D - L and I - J planes and the Fisher–Shannon and López–Mancini–Calbet (LMC) shape complexities. The analysis of the information-theoretical functionals of the one-particle density was computed in position (r) and momentum (p) space. The analysis revealed that all of the chemically significant regions can be identified from the information functionals and most of the information-theoretical planes, i.e. the reactant/product regions (R/P), the transition state (TS), including those that are not present in the energy profile such as the bond cleavage energy region (BCER), and the bond breaking/forming regions (B–B/F). The analysis of the complexities shows that, in position as well as in the joint space, the energy profile of the abstraction reaction bears the same information-theoretical features as the LMC and FS measures. We discuss why most of the chemical features of interest, namely the BCER and B–B/F, are lost in the energy profile and that they are only revealed when particular information-theoretical aspects of *localizability* (L or J), *uniformity* (D) and *disorder* (I) are considered.

Keywords: statistical complexity; Fisher information; information theory; chemical reactions

1. Introduction

In recent years there has been increasing interest in applying complexity concepts to study physical, chemical and biological phenomena. Complexity measures are understood as general indicators of pattern, structure, and correlation in systems or processes. Several alternative mathematical notions have been proposed for quantifying the concepts of complexity and information, including the Kolmogorov–Chaitin or algorithmic information theory [1], the classical information theory of Shannon and Weaver [2], Fisher information [3], and the logical [4] and the thermodynamical [5] depths, among others. Some of the above share rigorous connections with others as well as with Bayes and information theory [6]. The term complexity has been applied with different meanings: algorithmic, geometrical, computational, stochastic, effective, statistical, and structural, among others, and it has been employed in many fields: dynamical systems, disordered systems, spatial patterns, language, multi-electronic systems, cellular automata, neuronal

networks, self-organization, DNA analyses, social sciences, astrophysics, among others [7,8].

The definition of complexity is not unique, and its quantitative characterization has been an important subject of research and it has received considerable attention [9,10]. The usefulness of each definition depends on the type of system or process under study, the level of the description, and the scale of the interactions among either elementary particles, atoms, molecules, biological systems, etc. Fundamental concepts such as uncertainty or randomness are frequently employed in the definitions of complexity, although other concepts such as clustering, order, localization or organization might also be important for characterizing the complexity of systems or processes. It is not clear how the aforementioned concepts might intervene in the definitions so as to quantitatively assess the complexity of the system. However, recent proposals have formulated this quantity as a product of two factors, taking into account *order/disequilibrium* and *delocalization/uncertainty*. This is the case of the definition of the López–Mancini–Calbet

*Corresponding author. Email: esquivel@xanum.uam.mx

(*LMC*) shape complexity [9–12] that, like others, satisfies the boundary conditions by reaching its minimal value in the extreme ordered and disordered limits. The *LMC* complexity measure has been criticized [11], modified [12] and generalized [13], leading to a useful estimator that satisfies several desirable properties of invariance under scaling transformations, translation, and replication [14,16]. The utility of this improved complexity has been verified in many fields [8] and allows reliable detection of periodic, quasiperiodic, linear stochastic, and chaotic dynamics [14–16]. The *LMC* measure is constructed as the product of two important information-theoretic quantities (see below): the so-called disequilibrium D (also known as self-similarity [17] or information energy [18]), which quantifies the *departure of the probability density from uniformity* [12,15] (equiprobability), and the Shannon entropy S , which is a general measure of randomness/uncertainty of the probability density [2], and quantifies the *departure of the probability density from localizability*. Both *global* quantities are closely related to the measure of spread of a probability distribution.

The Fisher–Shannon product FS has been employed as a measure of atomic correlation [19] and is also defined as a statistical complexity measure [20]. The product of the power entropy J – explicitly defined in terms of the Shannon entropy (see below) – and the Fisher information measure I , combines both the global character (depending on the distribution as a whole) and the local character (in terms of the gradient of the distribution) to preserve the general complexity properties. Compared with the *LMC* complexity, apart from the explicit dependence on the Shannon entropy which serves to measure the uncertainty (localizability) of the distribution, the Fisher–Shannon complexity replaces the disequilibrium global factor D by the Fisher local factor to quantify the *departure of the probability density from disorder* [3] of a given system through the gradient of the distribution.

The Fisher information I itself plays a fundamental role in different physical problems, such as the derivation of the non-relativistic quantum-mechanical equations by means of the minimum I principle [3], as well as the time-independent Kohn–Sham equations and the time-dependent Euler equation [21]. More recently, the Fisher information has also been employed as an intrinsic accuracy measure for specific atomic models and densities [22] as well as for general quantum-mechanical central potentials [23]. The concept of phase-space Fisher information has been analysed for hydrogen-like atoms and the isotropic harmonic oscillator [24]. Several applications concerning atomic distributions in position and momentum space have been performed where the FS complexity

is shown to provide relevant information on atomic shell structure and ionization processes [20]. The Fisher measure has also been employed to test a density-based quantification of the steric effect of the ethane molecule [25].

On the other hand, theoretical chemistry has witnessed a great deal of research to study the energetics of chemical reactions [26]. For instance, a variety of calculations of potential energy surfaces have been performed at various levels of sophistication [27]. Within the broad scope of these investigations, particular interest has been focused on extracting information about the stationary points of the energy surface. Despite the fact that minima, maxima, and saddle points are useful mathematical features of the energy surface for following reaction paths [28], it has been difficult to attribute too much chemical or physical meaning to these critical points [29]. Whereas the reaction rate and the reaction barrier are chemical concepts that have been rigorously defined and experimentally studied since the early days of transition state (TS) theory [30], the structure of the TS remains a quest of physical organic chemistry. Understanding the TS is a fundamental goal of chemical reactivity theories, and implies knowledge of the chemical events that take place to better understand the kinetics and the dynamics of a reaction. On the other hand, a variety of density descriptors have been employed to study chemical reactions [30,31]. Among these, it is worth mentioning the reaction force studies on the potential energy of reactions that have been employed to characterize changes in the structural and/or electronic properties of chemical reactions [32,33]. In recent years, there has been increasing interest in the analysis of the electronic structure of atoms and molecules by applying information theory (IT) [34]. In recent studies we have shown that information-theoretic measures are capable of providing simple pictorial chemical descriptions of atoms and molecules. For instance, theoretic-information analyses have shown to be useful for the phenomenological description of the course of elementary chemical reactions through the localized/delocalized behavior of the electron densities in position and momentum space by revealing important chemical regions that are not present in the energy profile such as those in which bond forming and bond breaking occur and also the bond cleavage energy regions (BCER) [35]. Furthermore, the synchronous reaction mechanism of a S_N2 -type chemical reaction and the non-synchronous behavior of the simplest hydrogen abstraction reaction were predicted by use of Shannon entropies analysis [36]. Also, the chemical phenomenon of B–B/F was recently studied by the

125

130

135

140

145

150

155

160

165

170

175 Fisher information measure for both reactions, showing that this local measure in momentum space is highly sensitive in detecting these chemical events, whereas that in position space is able to detect differences in their mechanisms [37].

180 The goal of the present study is to perform an information-theoretical analysis of the hydrogenic abstraction reaction by use of information-theoretical measures and planes as well as the *LMC* and *FS* complexity products. Focus will be set on the recognition of patterns of *uncertainty/localizability, disorder/narrowness* and *disequilibrium/uniformity* through *S, I* and *D*, respectively. The organization of the paper is as follows. In Section 2 we defined the complexity measures along with their information-theoretic components. In Section 3 we calculate the information components as well as the Fisher–Shannon and *LMC* complexities. These information functionals of the one-particle density are computed in position (*r*), momentum (*p*) as well as in the joint product space (*rp*) that contains more complete information about the system. In addition, the Fisher–Shannon (*I–J*) and the disequilibrium–Shannon (*D–L*) and the Fisher–disequilibrium (*I–D*) planes are studied. In Section 4, some conclusions are given.

200

2. Information-theoretical measures and complexities

In the independent-particle approximation, the total density distribution in a molecule is a sum of the contributions from the electrons in each of the occupied orbitals. This is the case in both *r*-space and *p*-space, position and momentum, respectively. In momentum space, the total electron density, $\gamma(\vec{p})$, is obtained through the molecular momentals (momentum-space orbitals) $\varphi_i(\vec{p})$, and similarly for the position-space density, $\rho(\vec{r})$, through the molecular position-space orbitals $\phi_i(\vec{r})$. The momentals can be obtained by three-dimensional Fourier transformation of the corresponding orbitals (and conversely)

$$\varphi_i(\mathbf{p}) = (2\pi)^{-3/2} \int d\mathbf{r} \exp(-i\mathbf{p} \cdot \mathbf{r}) \phi_i(\mathbf{r}). \quad (1)$$

Standard procedures for the Fourier transformation of position space orbitals generated by *ab-initio* methods have been described [38]. The orbitals employed in *ab-initio* methods are linear combinations of atomic basis functions and since analytic expressions are known for the Fourier transforms of such basis functions [39], the transformation of the total molecular electronic wavefunction from position to momentum space is computationally straightforward [40].

As mentioned in the introduction, the *LMC* complexity is defined through the product of two relevant information-theoretic measures. For a given probability density in position space, $\rho(\vec{r})$, the *C(LMC)* complexity is given by [9–12]

$$C_r(LMC) = D_r e^{S_r} = D_r L_r, \quad (2)$$

where D_r is the disequilibrium [17,18],

$$D_r = \int \rho^2(\mathbf{r}) d\mathbf{r}, \quad (3)$$

and S is the Shannon entropy [2],

$$S_r = - \int \rho(\mathbf{r}) \ln \rho(\mathbf{r}) d^3\mathbf{r}, \quad (4)$$

from which the exponential entropy $L_r = e^{S_r}$ is defined. Similar expressions for the *LMC* complexity measure in the conjugated momentum space might be defined for a distribution $\gamma(\vec{p})$

$$C_p(LMC) = D_p e^{S_p} = D_p L_p. \quad (5)$$

It is important to mention that the *LMC* complexity of a system must comply with the following lower bound [41]:

$$C(LMC) \geq 1. \quad (6)$$

The *FS* complexity in position space, $C_r(FS)$, is defined in terms of the product of the Fisher information [3],

$$I_r = \int \rho(\mathbf{r}) \left| \vec{\nabla} \ln \rho(\mathbf{r}) \right|^2 d^3\mathbf{r}, \quad (7)$$

and the power entropy [20] in position space J_r ,

$$J_r = \frac{1}{2\pi e} e^{(2/3)S_r}, \quad (8)$$

which depends on the Shannon entropy defined above. Therefore, the *FS* complexity in position space is given by

$$C_r(FS) = I_r \cdot J_r, \quad (9)$$

and similarly

$$C_p(FS) = I_p \cdot J_p \quad (10)$$

in momentum space.

Let us remark that the factors in the power Shannon entropy J are chosen to preserve the invariance under scaling transformations, as well as the rigorous relationship [42]

$$C(FS) \geq n, \quad (11)$$

225

230

235

240

245

with n being the space dimensionality, thus providing a universal lower bound to FS complexity. The definition in Equation (8) corresponds to the particular case $n=3$, the exponent containing a factor $2/n$ for arbitrary dimensionality.

It is worth noting that the aforementioned inequalities remain valid for distributions normalized to unity, which is the choice that it is employed throughout this work for the three-dimensional molecular case.

Apart from the analysis of the position and momentum information measures, we have considered it useful to study these magnitudes in the product rp -space, characterized by the probability density $f(\vec{r}, \vec{p}) = \rho(\vec{r})\gamma(\vec{p})$, where the complexity measures are defined as

$$C_{rp}(LMC) = D_{rp}L_{rp} = C_r(LMC)C_p(LMC) \quad (12)$$

and

$$C_{rp}(FS) = I_{rp}J_{rp} = C_r(FS)C_p(FS). \quad (13)$$

From the above two equations, it is clear that the features and patterns of both the LMC and FS complexity measures in the product space will be determined by those of each conjugated space. However, the numerical analyses carried out in the next section reveal that the momentum space contribution plays a more relevant role than the position space contribution.

3. Complexity analysis of the hydrogenic abstraction reaction

The electronic structure calculations performed in the present study were carried out with the Gaussian 03 suite of programs [43]. Reported TS geometrical parameters for the abstraction reaction were employed [44]. Calculations for the IRC were performed at the MP2 (UMP2 for the abstraction reaction) level of theory with at least 35 points for each of the directions (forward/reverse) of the IRC. A high level of theory and a well-balanced basis set (diffuse and polarized orbitals) were then chosen to determine all of the properties for the chemical structures corresponding to the IRC. Thus, the QCISD(T) method was employed in addition to the 6-311++G** basis set, unless otherwise stated. The molecular information measures were S , D , I and J , the information planes ($D-L$), ($I-J$) and ($I-D$) and the complexity measures were $C(LMC)$ and $C(FS)$. All information-theoretical quantities are calculated in position and momentum space for the IRC path of the abstraction reaction and obtained by employing software developed in our laboratory along

with 3D numerical integration routines [45], and the DGRID suite of programs [40].

The reaction $H^\bullet + H_2 \rightarrow H_2 + H^\bullet$ is the simplest radical abstraction reaction involving a free radical (atomic hydrogen) as a reactive intermediate. This kind of reaction involves at least two steps (S_N1 reaction type): in the first step, a new radical (atomic hydrogen in this case) is created by homolysis, and in the second step the new radical recombines with another radical species. Such homolytic bond cleavage occurs when the bond involved is not polar and there is no electrophile or nucleophile at hand to promote heterolytic patterns. The bond-breaking process requires energy that should be dissipated by relaxing the structure at the TS. Evidence has been presented [36] that shows that the two-step mechanism observed for this type of reaction is completely characterized by the Shannon entropies in conjugated space through concerted but yet asynchronous behavior.

Our calculations for this reaction were performed at two different levels: the IRC was obtained at the UMP2/6-311G level, and all properties at the IRC were obtained at the QCISD(T)/6-311++G** level of theory. As a result of the IRC, 72 points evenly distributed between the forward and reverse directions of the IRC were obtained. A relative tolerance of 1.0×10^{-5} was set for the numerical integrations [45].

Insight into the structural features of the distributions in both spaces concerning the global spreading (*delocalization*) of the densities can be obtained through the Shannon entropies in conjugated space. The behavior of the densities related to their local changes is appropriately described by a measure such as the Fisher information [3]. This measure quantifies the pointwise concentration of the electronic probability cloud, for each space, by means of the gradient content of the electron distribution, thus revealing the changes of the density and providing a quantitative estimation of its oscillatory character (smoothness). It is worth mentioning that, due to the global or local character of the particular information measure to be employed for the analysis, it is clear that each is capable of a partial description of all chemical phenomena, i.e. detection of the R/P (reactant/product complexes) regions, B-B/F (bond-breaking/forming) regions, BCER, TS, mechanistic behavior, etc. Therefore, in order to allow for a full characterization of a chemical process it would be necessary to perform a complexity analysis because these information-theoretical products provide complementary information sources, i.e. D (departure from *uniformity*) with L (departure from *localizability*) through the $C(LMC)$ measure and also I (departure from *disorder*) with J (departure from *localizability*) through

295

300

305

310

315

320

325

330

335

340

345

the $C(FS)$ measure (Equations (2), (5), (9) and (10)).

350 In the following sections we employ global and local
quantities to provide a complete description of the
hydrogenic abstraction reaction.

3.1. Information measures

355 Figure 1 depicts the values for the Shannon entropies
in conjugated space so as to provide a description of
the abstraction reaction in terms of the localizability
features of the densities in conjugated space which will
be of utility for analysing its complexity behavior. Both
 $C(LMC)$ and $C(FS)$ employ this global measure from
360 the definition of L and J , respectively. Summarizing
the analysis performed in Ref. [35], the phenomeno-
logical description of the reaction shows the following:
as the molecular complex approaches the TS its
position space density becomes localized (minima of
365 the position space density) in preparation for bond
rupture, a process that requires energy. This is revealed
by the local maxima of the corresponding momentum
densities, i.e. its delocalization indicates a local increase
of the necessary kinetic energy for bond cleavage at the
BCER (bond cleavage energy regions) as observed in
370 Figure 1. The homolysis then provokes energy/density
relaxation of the molecules towards the TS, which is
also observed from the figure.

We have found it useful to describe the chemical
375 process in terms of the local/global features of the
distributions at the IRC through the local measure
 I (departure from disorder) and through the global
measure D (departure from uniformity). Therefore, in
Figures 2 and 3 we depict both the Fisher information
and the disequilibrium measures, in position and
380 momentum space, respectively. Alluding to a previous
study [37], a phenomenological description of the
chemical course shows the following local features.
Fisher information in position space (Figure 2) shows
maxima at the R/P region, whereas it has a global
minimum at the TS, i.e. as the reactant complex
approaches the TS the *disorder* of the distributions in
position space increases. This may be interpreted
chemically as follows: as the reaction evolves, the
385 structural changes in the distributions diminish, which
means that the R/P has larger changes than the TS,
which is characterized by a symmetric distribution (the
smoothest of all at the IRC) produced by the spin
coupling of the hydrogenic radical species. It is
390 interesting to note that the gradient of the distribu-
tions increases towards the BCER at -1.0 a.u., indicat-
ing the beginning of the bond-cleavage region. Continu-
ing with the analysis from Figure 2, the global fea-
395 tures of the chemical course of the reaction indicate that the

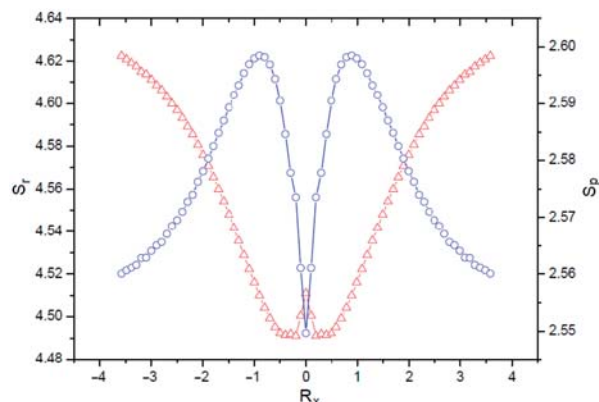


Figure 1. Shannon entropies in conjugated spaces S_r (red triangles) and S_p (blue circles) for the IRC of the abstraction reaction.

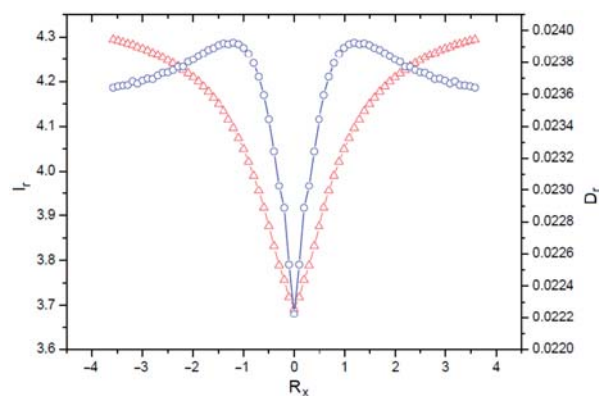


Figure 2. Fisher information measure (red triangles) and disequilibrium (blue circles) in position space for the IRC of the abstraction reaction.

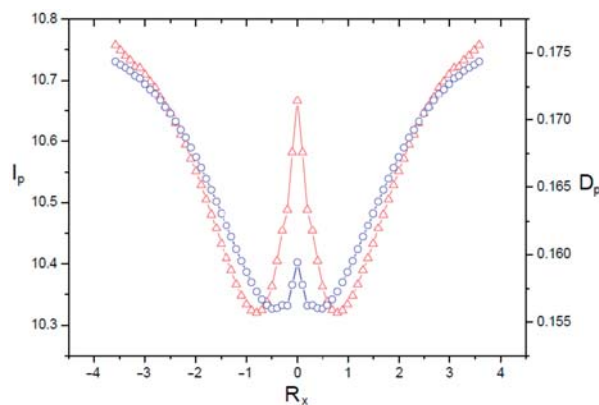


Figure 3. Fisher information measure (red triangles) and disequilibrium (blue circles) in momentum space for the IRC of the abstraction reaction.

400 disequilibrium for the R/P show lower values than
the BCER and that the TS has a global minimum,
i.e. the position space distributions are the least
uniform at the BCER, whereas the largest *uniformity*
405 is observed at the TS. Chemically, the reaction
proceeds by deforming the densities in the R/P region
so as to reach maxima at the BCER, i.e. position space
densities at the onset of the bond-cleavage regions are
the least *uniform*. These regions are also associated
410 with the most *delocalized* densities in momentum space
according to the Shannon entropy (see Figure 1), hence
corresponding to the most energetic structures at the
IRC [35]. As mentioned above the reaction proceeds in
two steps; at the end of the bond-cleavage process the
415 TS is reached during the first stage and, according to
Figure 2, the TS is characterized by the most *uniform*
distribution. It is worth noting that the R/P along with
the TS show smaller values for D compared with the
BCER, which are associated with more *equiprobable*
structures (position space densities). Summarizing, the
420 reaction may be characterized in terms of *uniformity*
through the disequilibrium measure in position space
in that its maxima correspond to the BCER and the
global minimum to the TS.

The local/global features of the course of the
425 chemical reaction are complemented with the analysis
of I and D in momentum space. Alluding to previous
work [37] we observe that Fisher information may
describe the *disorder* features of the reaction: the R/P
as well as the TS show the largest values, indicating
430 more *ordered* structures (momentum space densities)
corresponding to the most *localized* structures
(see Figure 1), whereas the BCER are associated with
the most *disordered* structures, associated, in turn,
with the most *delocalized* structures and hence the
435 more energetic structures [35]. In physical terms,
the R/P and TS exert larger energetic changes
than the BCER so as to accumulate the necessary
energy for bond breaking at -1.0 a.u. in the first step
of the reaction (which is completed when the bond is
440 formed beyond the TS in the second stage [35]). At the
onset of this region the process reverts by releasing the
accumulated energy at the TS when bond cleavage is
completed and then a more *ordered* structure with a
larger energetic change is observed. The reaction
445 continues in the second step so as to accumulate
energy in the bond-forming stage and then releases it to
reach the product complex. The global features of the
reaction are depicted in Figure 3 through the disequi-
librium measure, which shows that the R/P possess the
450 least *uniform* momentum space densities of the remain-
der at the IRC, whereas the B-B/F regions [35] have
the most *uniform* ones. The TS structure shows a local
maximum with a less *uniform* momentum density.

The chemical significance of these features is that the
455 structure of the R/P is deformed so as to reach a higher
degree of *uniformity* at the B-B/F regions, which are
associated with highly *localized* densities in position
space according to the Shannon entropies depicted in
Figure 1. The process then reverts so as to increase the
460 disequilibrium (less *uniformity*) to reach the TS. It is
interesting to observe that both processes (bond
breaking and TS forming in the forward direction of
the IRC) are located within the energy-releasing region
described above for the Fisher measure, which means
465 that both processes require energy. Interestingly, the
structural energetic change to reach the TS is more
pronounced than that required for bond breaking.
This is because this reaction is driven by a spin
coupling mechanism as a unique source of change.
470 In the second step of the reaction the process is
inverted and the energy accumulation region shown by
Fisher in Figure 3 is now employed to leave the
structural equiprobability (*uniformity*) in position
space (D in Figure 2) implied by the TS. This is
475 shown in Figure 3 by passing from structural disequi-
librium to *uniformity* in momentum space (maximum
and minimum values for D at the TS and bond-
forming regions, respectively). The process then reverts
by releasing the energy necessary for the structural
480 deformation of the distribution in momentum space by
diminishing the *uniformity*. It is worth mentioning that
the reaction (in momentum space) might be character-
ized in terms of *uniformity* through the disequilibrium
measure in that its minima describe the B-B/F regions
485 and the local maximum is associated with the TS.

3.2. Information planes

In the search of any joint features of *disorder–*
uniformity (I – D), *uniformity–localizability* (D – L), and
disorder–localizability (I – J) for the chemical course of
490 the reaction we have found it useful to plot the
contribution of I and D to the I – D plane, of D and L
to the total LMC complexity, and similarly of I and J
to the FS complexity.

Notwithstanding that not all information products
495 are good candidates to form complexity measures,
i.e. to preserve the desirable properties of invariance
under scaling, translation and replication, we have
found it interesting to study the plane I – D , with the
purpose of analysing patterns of *disorder–uniformity*.
500 In Figures 4 and 5 we give a phenomenological
description of the reaction through the I_r – D_r and
 I_p – D_p planes, respectively. In position space (Figure 4)
we note that, at the R/P, the *order* is maximum and,
as the reaction develops, both the *disorder* and

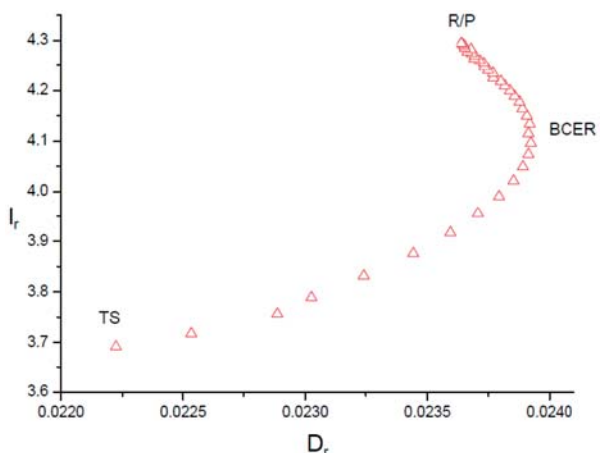


Figure 4. Fisher–disequilibrium plane in position space for the IRC of the abstraction reaction.

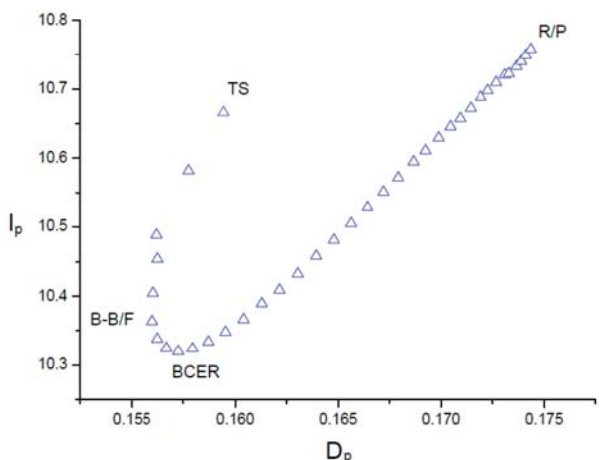


Figure 5. Fisher–disequilibrium plane in momentum space for the IRC of the abstraction reaction.

the Fisher measure, then the process reverts and the structural changes increase so as to reach the product complex. This effect is accompanied by a distortion of the position space densities so as to decrease/increase (depending on the direction of the reaction) their *uniformity* with the bending located at the BCER as the reaction evolves from the reactant complex up to the TS and then the process reverts at this point, i.e. the distortions acquire opposite directions by augmenting/reducing (depending on the direction of the reaction) its disequilibrium so as to reach the product complex with the same inflexion point at the BCER.

In momentum space the R/P regions exhibit maximum values for I and D (*order* and *disequilibrium*) and, as the reaction develops (forward direction), both quantities diminish so as to reach the BCER, which possesses maximum *disorder*, then the *order* increases by reducing D up to the B–B/F region, which has a minimum D value, towards the TS, which has maximum local *order*. The general observation from Figure 5 is that the *disorder/uniformity* ratio possesses a positive slope, which is remarkably linear from R/P to BCER, so that both quantities increase until the BCER is reached and then the slope becomes larger at the B–B/F region with both quantities decreasing so as to reach the TS. In chemical terms, the structural changes that the momentum space distributions exert decrease as the reaction evolves (forward direction), which conveys an energy accumulation (see analysis of Figure 3) up to where the BCER is reached, and then the process reverts by releasing energy with an increase in structural changes up to the TS. These energetic effects are accompanied by structural distortions in momentum space so as to increase the *uniformity* when the energy is accumulated from R to BCER, and then, as the energy is released, the distortions exert two opposite changes from BCER to TS, as explained below. According to the Fisher measure, from the BCER to the TS, the reaction requires energy, and judging by the D measure, the reaction involves two stages: bond breaking and spin coupling, as we have explained in connection with Figure 3. This is clearly observed when structural *uniformity* increases from BCER to a global minimum at B–B/F, and from this point the *uniformity* decreases so as to reach the TS.

It is worth comparing Figures 4 and 5 with respect to the behavior of the complementarity of the different spaces in the course of the chemical reaction. In position space (Figure 4) we observe that the BCER is characterized by minimum uniformity, whereas in momentum space (Figure 5) this region characterizes a state of maximum disorder. In both cases, one can note that the BCER reflects an inflexion point, although the behavior in position space is that

505 the *disequilibrium* increase until the BCER is reached. At this point the *disequilibrium* is maximum and then both the *disorder* and the *uniformity* increase until the TS is reached. At the TS, both the *order* and the *disequilibrium* are minimum. It is worth noting that the B–B/F region is not present in this plane. A general observation from Figure 4 is that the *order/uniformity* ratio possesses a negative slope that is nearly linear from R/P to BCER, so that both quantities decrease until the BCER is reached and, at the same time, the *order/disequilibrium* ratio has a positive slope, indicating that both quantities decrease so as to reach the TS. Chemically, one may observe from Figure 4 that the structural changes in position space diminish along the IRC as the reaction evolves and the reactant complex reaches the TS, judging by

525

530

535

540

545

550

555

560

565

570

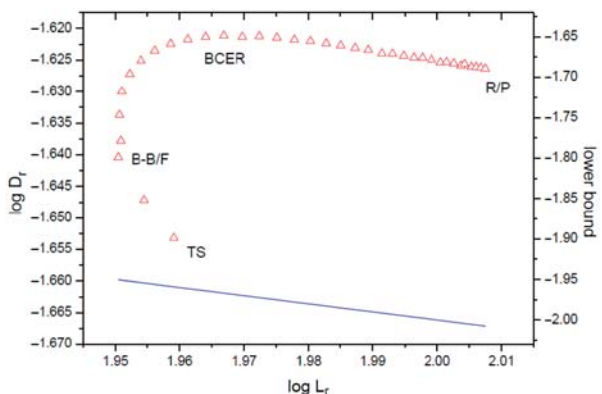


Figure 6. Disequilibrium–Shannon plane ($D-L$) in position space (red triangles) for the IRC of the abstraction reaction on a double logarithmic scale. The lower bound is depicted by the blue line (Equation (6)).

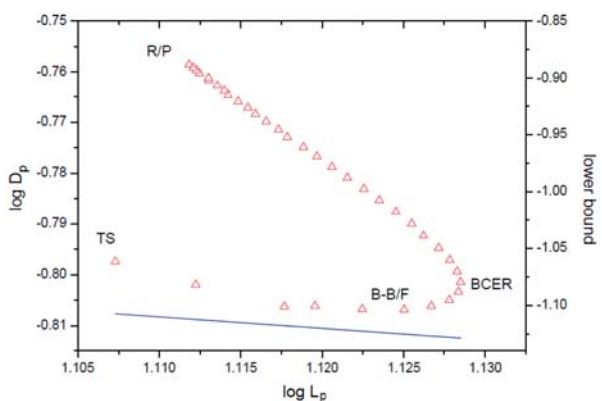


Figure 7. Disequilibrium–Shannon plane ($D-L$) in momentum space (red triangles) for the IRC of the abstraction reaction on a double logarithmic scale. The lower bound is depicted by the blue line (Equation (6)).

showing that an increase (decrease) in *uncertainty*, L , along them is compensated by a proportional decrease (increase) in disequilibrium, and greater deviations from this frontier are associated with greater *LMC* complexities.

From Figure 6 we note that, from the R/P to the BCER regions, the behavior is isocomplex with the $C(LMC)$ bound, whereas for the rest of the IRC it behaves in a more complex manner. The general observations are that the R/P show maximum *uncertainty* (highly delocalized structures) and, as the reaction evolves, both *uniformity* and *uncertainty* decrease up to the BCER, which exhibits maximum *disequilibrium*. Then *uncertainty* follows its decreasing path, whereas *uniformity* increases up to the B–B/F region, which exhibits minimum *uncertainty* (highly localized structures) up to the TS by reducing the *disequilibrium* at the expense of increasing *uncertainty* so as to reach a structure with maximum *uniformity*. The chemical analysis proceeds by noting that, as the reaction develops (forward direction), the position space structures become distorted by losing *uniformity* and gaining *localizability* up to the BCER in preparation for bond cleavage. Then, from the BCER up to the B–B/F region, we also observe two stages of the mechanism: first, the structures acquire both greater *localizability* and greater *uniformity* for bond rupture at the B–B/F. In the second stage, from B–B/F to the TS, spin coupling is achieved by gaining *uniformity* at the expense of augmenting *uncertainty*.

In momentum space (Figure 7) we observe fairly isocomplex behavior from R/P to BCER. In addition, the R/P are characterized by possessing maximum disequilibrium and, as the reaction evolves, *uniformity* increases by augmenting the *uncertainty* up to the BCER, which has structures with maximum *delocalizability*. Then the structures gain more *uniformity* at the expense of lowering its *uncertainty* at the B–B/F, which has the maximum *uniformity*. From this region up to the TS, *uncertainty* keeps diminishing at the expense of losing *uniformity*. The energetic analysis of Figure 7 completes the chemical picture by noting that, from R/P to BCER, the structural changes exert an increase in *delocalizability*, and hence energy is being accumulated. The opposite is observed from BCER up to TS, where the structural changes are those that augment its *localizability*, hence releasing energy. As mentioned above, two stages are also observed from BCER to B–B/F and from this region to the TS, i.e. for bond breaking, *uncertainty* decreases at the expense of gaining *uniformity*, and for spin coupling in the second stage, it not only requires a decrease of *uncertainty* but also a reduction in *uniformity*.

575 of reaching a state of maximum disorder and uniformity together, whereas in momentum space the course of the reaction points to a state of local minimum disorder at the TS.

580 Figures 6 and 7 show plots (on a double-logarithmic scale) of the D_r-L_r and D_p-L_p planes for the chemical reaction. At this point it is worth mentioning that there is a rigorous lower bound to the associated $C(LMC)$ complexity, given by Equation (6), which is $C(LMC) = D \cdot L \geq 1$ for both spaces.
585 From both figures we can see that the $D-L$ plane is clearly separated into two regions, according to the $D \cdot L \geq 1$ inequality (valid for position, momentum as well as product spaces), and the region below the line (equality) corresponds to the forbidden region. Parallel lines to this bound represent isocomplexity regions,
590

595

600

605

610

615

620

625

630

635

640

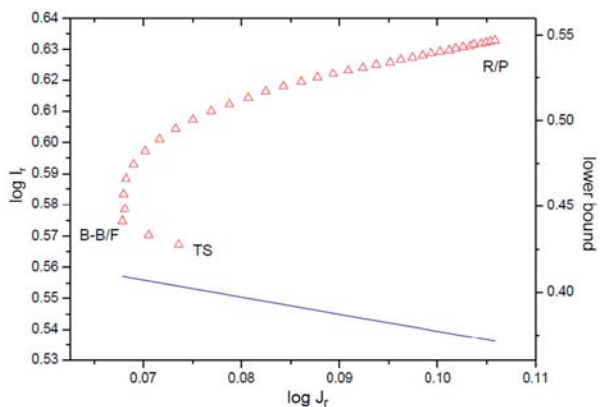


Figure 8. Fisher-Shannon plane (I - J) in position space (red triangles) for the IRC of the abstraction reaction on a double logarithmic scale. The lower bound is depicted by the blue line (Equation (11) with $n = 3$).

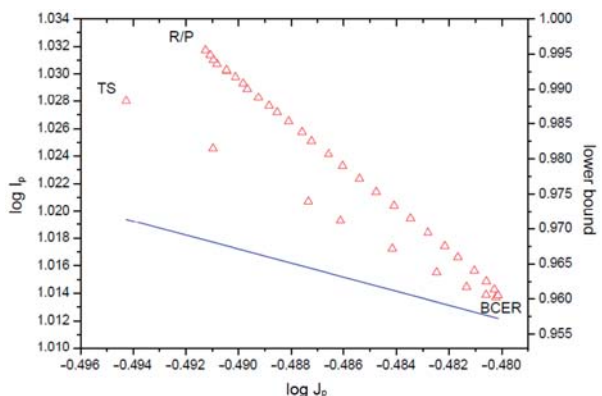


Figure 9. Fisher-Shannon plane (I - J) in momentum space (red triangles) for the IRC of the abstraction reaction on a double logarithmic scale. The lower bound is depicted by the blue line (Equation (11) with $n = 3$).

The complementarity of the conjugated spaces, r and p , in the course of the chemical reaction can be analysed from Figures 6 and 7. The general observation from these figures is that they reflect opposite behavior, i.e. for each of the most representative regions in the reaction (R/P, BCER, etc.) we observe states of maximum delocalizability in position space (Figure 6) corresponding to minimum uniformity in momentum space (Figure 7).

Figures 8 and 9 show plots (on a double-logarithmic scale) of the I_r - J_r and I_p - J_p planes for the chemical reaction. At this point it is worth mentioning that there is a rigorous lower bound to the associated $C(FS)$ complexity, given in Equation (6), which is $C(FS) = I \cdot J \geq 3$ for both spaces.

In position space, Figure 8 indicates a division of the I_r - J_r plane into two regions where the straight line $IJ=3$ (drawn in the plane on a logarithmic scale) divides it into an ‘allowed’ (upper) and a ‘forbidden’ (lower) part. In position space (Figure 8) the R/P are characterized by maximum values for *order* and *uncertainty*. As the reaction proceeds, *disorder* increases at the expense of decreasing *uncertainty* from the R/P to the B-B/F regions. The latter has highly *localized* densities, and *disorder* maintains its decreasing path at the expense of augmenting its *uncertainty* from the B-B/F to the TS. It is worth mentioning that the BCER are not present in this plane. Chemically, along the IRC we observe monotonically decreasing behavior for Fisher information, although the structural changes for the position space densities diminish more significantly from the R/P to the B-B/F regions than the changes from B-B/F to the TS. These changes are accompanied by an increase in structural *localizability* from the R/P to the B-B/F regions and, from this point to the TS, the opposite is observed, i.e. the TS has a more *delocalized* position space density.

Figure 9 depicts the corresponding measures for the I_p - J_p plane and some general aspects can be noted: (i) remarkable isocomplex behavior (linearity), which is divided into two regions, from R/P to BCER, and from BCER to the TS, and (ii) the B-B/F region is missing from this plane. In addition, we note from Figure 9 that the R/P are characterized by maximum structural *order* in momentum space that diminishes up to the BCER, which has maximum *disorder* and maximum *uncertainty*. This behavior then reverts and the *uncertainty* as well as the *disorder* of the process from BCER up to the TS decrease. This last point possesses the minimum global *uncertainty*. From a chemical point of view, the process behaves in such a way that, from R/P to BCER, energy is accumulated by gradually *delocalizing* the momentum space densities. The opposite is observed from BCER to the TS regions, where energy is released in order to achieve the bond cleavage and the spin coupling processes as discussed above.

For the I - J plane the behavior of the conjugated spaces in the course of the reaction appears to be more complex, in that not all the regions are fully characterized in both spaces as commented on above. In position space (Figure 8), localizability increases from the R/P to the B-B/F regions, whereas in momentum space (Figure 9) it diminishes from R/P to BCER. The opposite is observed from the B-B/F to the TS in that the localizability diminishes in position space, whereas in momentum space it increases from the BCER to the TS.

3.3. Complexities

In the search for joint patterns of *uniformity–localizability* through $C(LMC)$ and *disorder–localizability* through $C(FS)$ we show in Figures 10 and 11 the values for these complexity measures in position and momentum space, respectively. The general observation from Figure 10 is that both complexity measures behave similarly in position space. It can be observed that the R/P regions have maximum complexity and, as the reaction evolves, both complexities diminish up to the TS, which has the minimum complexity value at the IRC. It is worth noting that both measures fail to detect the BCER and B–B/F regions.

In momentum space the $C(LMC)$ measure looks very much like that in position space, i.e. maximum values for the R/P regions and minimum for the TS, and failing to detect the BCER and B–B/F regions. The situation for the Fisher–Shannon measure is different. As the reaction evolves, complexity decreases from maximum values at the R/P regions up to the B–B/F regions, which have the minimum values, and the complexity increases so as to reach the TS. It is interesting to note that whereas the joint measure for I_p and J_p is able to detect the B–B/F regions, neither of these two separate measures reveal it, as observed from Figures 1 and 3.

At this stage of the analysis we have managed with valuable data to establish a relationship between the information-theoretical features of the reaction studied in the present work and that of the total energy at its IRC profile. Thus, Figures 12–14 depict the $C(LMC)$ and $C(FS)$ complexity values as a function of energy for the conjugated spaces and for the product space, respectively.

Figure 12 shows monotonic decreasing behavior for both complexity measures (in position space) versus energy, i.e. as the reaction evolves the complexity diminishes at the expense of augmenting the energy up to the TS, which is shown at the bottom right corner of the figure. Further, our results show fairly linear behavior along the IRC except for the region in the vicinity of the R/P. Hence, we note that, in position space, the energy profile of the abstraction reaction bears the joint features of $C(LMC)$ (uniformity–localizability) and $C(FS)$ (disorder–localizability).

Also, the information-theoretic features of *uniformity–localizability* in momentum space shown by $C(LMC)$ in Figure 13 appear to describe the behavior of the total energy to a very good extent, except for a small region close to the R/P. In contrast, the $C(FS)$ measure behaves in a more complex manner with respect to the energy, and does not reflect the

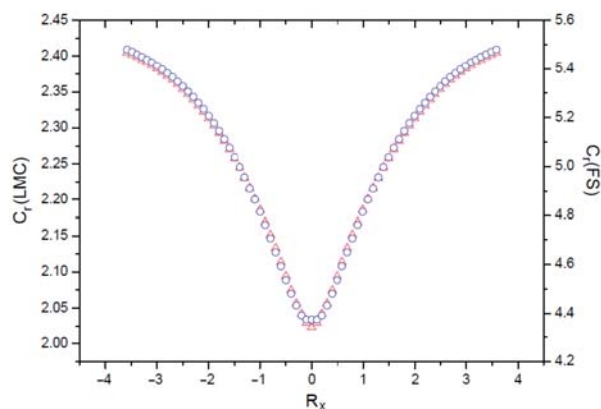


Figure 10. $C(LMC)$ (red triangles) and $C(FS)$ (blue circles) in position space for the IRC of the abstraction reaction.

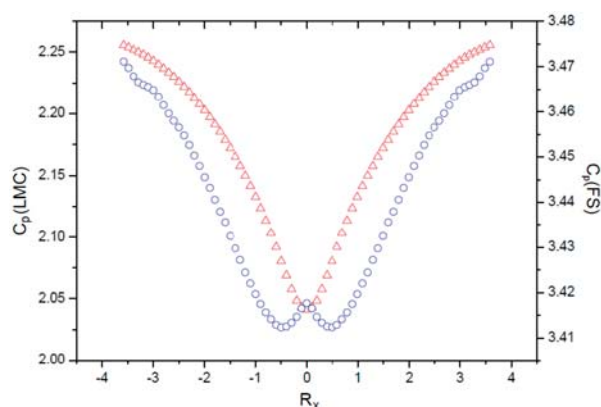


Figure 11. $C(LMC)$ (red triangles) and $C(FS)$ (blue circles) in momentum space for the IRC of the abstraction reaction.

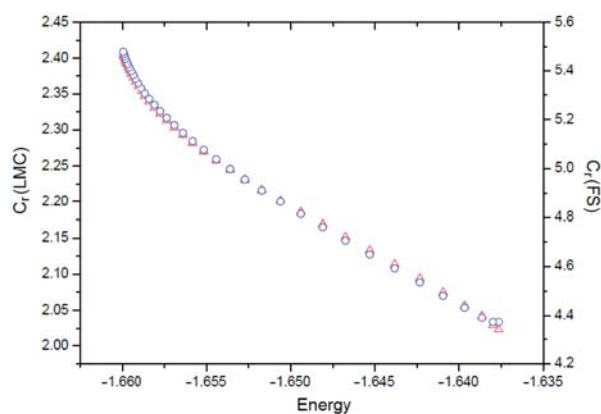


Figure 12. $C(LMC)$ (red triangles) and $C(FS)$ (blue circles) in position space as a function of the total energy of the abstraction reaction.

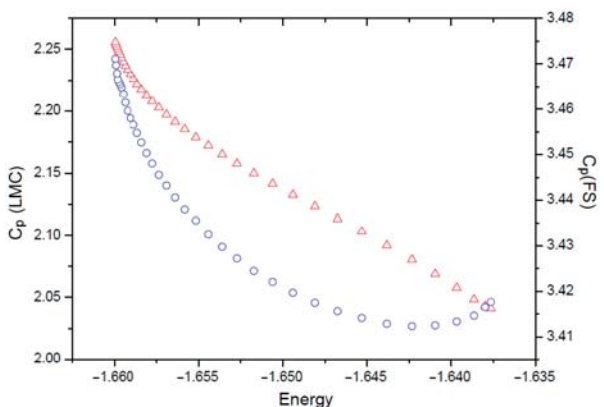


Figure 13. $C(LMC)$ (red triangles) and $C(FS)$ (blue circles) in momentum space as a function of the total energy of the abstraction reaction.

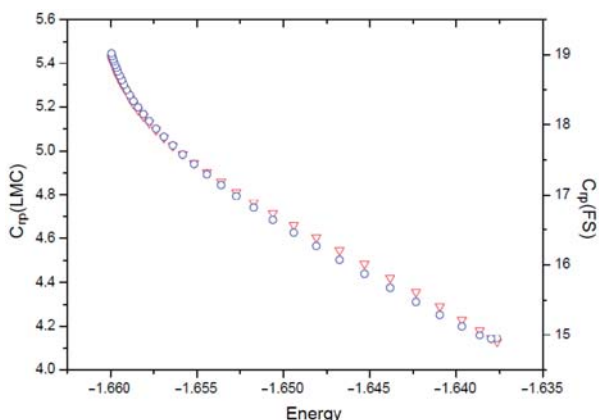


Figure 14. $C(LMC)$ (red triangles) and $C(FS)$ (blue circles) in the product space $r-p$ as a function of the total energy of the abstraction reaction.

765 B–B/F aspects of the reaction, which are indeed revealed by $C(FS)$.

770 It is interesting to collect together all the information-theoretical features analysed in this work through the complexities $C(LMC)$ and $C(FS)$ in product space to obtain a description of the energy profile for the abstraction reaction. As can be seen from Figure 14, the energy profile exhibits features of *uniformity–localizability* and *disorder–localizability* in the joint space. Therefore, it seems
775 feasible that most of the chemical features of interest, namely the BCER and the B–B/F, are lost in the energy profile. As observed above, these features are revealed only when the particular information-theoretical aspects of *uniformity*, *localizability* and
780 *disorder* are considered.

4. Conclusions

In this work, we have investigated the complexity of the hydrogenic abstraction reaction by means of information functionals D , L , I and J and joint information-theoretic measures, i.e. the $I-D$, $D-L$ and $I-J$ planes and the *Fisher–Shannon* and *LMC shape* complexities. 785

The analysis of the information-theoretical functionals of the one-particle density was performed in position (r) and momentum (p) space. These measures were found to reveal all the chemically significant aspects of the course of the reaction, i.e. the reactant/product region, the bond-cleavage energy region, the bond-breaking/forming region and the transition state. In addition, the information-theoretical concepts of *uniformity*, *disorder* and *localizability* were used to reveal the chemical phenomena of energy accumulation/release and to identify the mechanisms for bond forming and spin coupling. 790

In addition, the Fisher–disequilibrium ($I-D$), the *LMC* ($D-L$) and the Fisher–Shannon ($I-J$) planes were studied to identify informational aspects of *disorder–uniformity*, *uniformity–localizability* and *disorder–localizability*. The analysis revealed that all of the chemically significant regions can be identified from most information-theoretical planes as well as the energetic course of the reaction. It was found that although some planes are linear to the bounds of isocomplexity, the behavior of the reaction presents more complex patterns for some regions. 800

The complementarity of the conjugated spaces is manifest in a complex manner, i.e. for the planes we observe opposite behavior for some regions located between the chemically significant zones of the reaction, i.e. the R/P, BCER, B–B/F and the TS. However, these features are not completely characterized in the $I-J$ planes (nor in the complexities) so as to clearly observe opposite behavior of the conjugated spaces. On the other hand, it may be noted that position space information measures and complexities are closely related to the structural changes of the reactive complex along the IRC (e.g., B–B/F), whereas those in momentum space are associated with kinetic energetic changes (e.g., BCER). 805

810 It is important to mention that the local behavior of the Fisher information measure, as calculated by $C(FS)$ in momentum space, is the only complexity measure that can describe the B–B/F region, as compared with the other global measures which only reveal the R/P and TS. 815

820 According to the analysis of the complexities we note that, in position as well as in the joint space, the energy profile of the abstraction reaction bears the 825 830

joint information-theoretical features of uniformity–localizability through $C(LMC)$ and disorder–localizability through $C(FS)$. Finally, it is feasible that most of the chemical features of interest, namely the BCER and the B–B/F, are lost in the energy profile; these features are revealed solely when the particular information-theoretical aspects of D , L or J , and I are considered.

The results of this study indicate that further investigations are necessary in order to improve our understanding of the complexity of chemical reactions along the lines of analysing different reaction mechanisms, other information functionals, more intricate aspects of the energy profile, etc. We believe that the strategy followed in this study might be useful in more complex cases by describing the phenomenological behavior of the chemical probe concerning local and global features by use of three key information measures, i.e. Shannon, Fisher and disequilibrium. The information planes and complexity measures of the process might then be resolved in a feasible manner.

Acknowledgements

We wish to thank José María Pérez-Jordá and Miroslav Kohout for kindly providing their numerical codes. R.O.E. wishes to thank Juan Carlos Angulo and Jesús Sánchez-Dehesa for their kind hospitality during his sabbatical stay at the Departamento de Física Atómica, Molecular y Nuclear and the Instituto Carlos I de Física Teórica y Computacional at the Universidad de Granada, Spain. We acknowledge financial support via Mexican grants from CONACyT, PIFI and PROMEP-SEP and Spanish grants MICINN projects FIS-2008-02380, FQM-4643 and P06-FQM-2445 of Junta de Andalucía. J.A., J.C.A., J.S.D., and R.O.E. belong to the Andalusian research group FQM-0207. R.O.E. wishes to acknowledge financial support from the Ministerio de Educación of Spain through grant SAB2009-0120. Allocation of supercomputing time from Laboratorio de Supercomputo y Visualización at UAM, Sección de Supercomputacion at CSIRC Universidad de Granada, and Departamento de Supercomputo at DGSCA-UNAM is gratefully acknowledged.

References

- [1] A.N. Kolmogorov, *Probl. Inf. Transm.* **1**, 3 (1965); G. Chaitin, *J. ACM* **13**, 547 (1966).
- [2] C.E. Shannon and W. Weaver, *The Mathematical Theory of Communication* (University of Illinois Press, Urbana, 1949).
- [3] R.A. Fisher, *Proc. Cambridge Philos. Soc.* **22**, 700 (1925); B.R. Frieden, *Science from Fisher Information* (Cambridge University Press, Cambridge, 2004).

- [4] C.H. Bennet, in *The Universal Turing Machine a Half Century*, edited by R. Herhen (Oxford University Press, Oxford, 1988), pp. 227–257. 885
- [5] S. Lloyd and H. Pagels, *Ann. Phys. (N.Y.)* **188**, 186 (1988).
- [6] P.M.B. Vitanyi and M. Li, *IEEE Trans. Inf. Theory* **46**, 446 (2000). 890
- [7] C.R. Shalizi, K.L. Shalizi and R. Haslinger, *Phys. Rev. Lett.* **93**, 118701 (2004); M. Lovallo and L. Telesca, *J. Stat. Mech.* P03029 doi: 10.1088/1742-5468/2011/03/P03029 (2011); S.L. Zhang and T.M. Wang, *J. Biomol. Struct. Dynam.* **28**, 247 (2010); C.C. Moustakidis, V.P. Psonis, K.C. Chatzisavvas, C.P. Panos and S.E. Massen, *Phys. Rev. E* **81**, 011104 (2010); R. Lopez-Ruiz, A. Nagy, E. Romera and J. Sanudo, *J. Math. Phys.* **50**, 123528 (2009); S. Lopez-Rosa, J. Montero, P. Sanchez-Moreno, J. Venegas and J.S. Dehesa, *J. Math. Chem.* **49**, 971 (2011). 895
- [8] O.A. Rosso, M.T. Martin and A. Plastino, *Physica A* **320**, 497 (2003); K.Ch. Chatzisavvas, Ch.C. Moustakidis and C.P. Panos, *J. Chem. Phys.* **123**, 174111 (2005); A. Borgoo, F. De Proft, P. Geerlings and K.D. Sen, *Chem. Phys. Lett.* **444**, 186 (2007). 905
- [9] D.P. Feldman and J.P. Crutchfield, *Phys. Lett. A* **238**, 244 (1998).
- [10] P.W. Lamberti, M.T. Martin, A. Plastino and O.A. Rosso, *Physica A* **334**, 119 (2004). 910
- [11] C. Anteonodo and A. Plastino, *Phys. Lett. A* **223**, 348 (1996).
- [12] R.G. Catalán, J. Garay and R. López-Ruiz, *Phys. Rev. E* **66**, 011102 (2002); M.T. Martin, A. Plastino and O.A. Rosso, *Phys. Lett. A* **311**, 126 (2003). 915
- [13] R. López-Ruiz, *Biophys. Chem.* **115**, 215 (2005).
- [14] T. Yamano, *J. Math. Phys.* **45**, 1974 (2004).
- [15] R. López-Ruiz, H.L. Mancini and X. Calbet, *Phys. Lett. A* **209**, 321 (2000). 920
- [16] T. Yamano, *Physica A* **340**, 131 (1995).
- [17] R. Carbó-Dorca, J. Arnau and L. Leyda, *Int. J. Quantum Chem.* **17**, 1185 (1980).
- [18] O. Onicescu, *C.R. Acad. Sci. Paris A* **263**, 25 (1966).
- [19] E. Romera and J.S. Dehesa, *J. Chem. Phys.* **120**, 8906 (2004). 925
- [20] J.C. Angulo, J. Antolín and K.D. Sen, *Phys. Lett. A* **372**, 670 (2008); K.D. Sen, J. Antolín and J.C. Angulo, *Phys. Rev. A* **76**, 032502 (2007); J.C. Angulo and J. Antolín, *J. Chem. Phys.* **128**, 164109 (2008); J. Antolín and J.C. Angulo, *Int. J. Quantum Chem.* **109**, 586 (2009). 930
- [21] A. Nagy, *J. Chem. Phys.* **119**, 9401 (2003); R. Nalewajski, *Chem. Phys. Lett.* **372**, 28 (2003).
- [22] A. Nagy and K.D. Sen, *Phys. Lett. A* **360**, 291 (2006); K.D. Sen, C.P. Panos, K.Ch. Chatzisavvas and Ch. Moustakidis, *Phys. Lett. A* **364**, 286 (2007). 935
- [23] E. Romera, P. Sánchez-Moreno and J.S. Dehesa, *J. Math. Phys.* **47**, 103504 (2006); J.S. Dehesa, R. González-Férez and P. Sánchez-Moreno, *J. Phys. A* **40**, 1845 (2007). 940
- [24] I. Hornyak and A. Nagy, *Chem. Phys. Lett.* **437**, 132 (2007).

- [25] R.O. Esquivel, S. Liu, J.C. Angulo, J.S. Dehesa, J. Antolin and M. Molina-Espiritu, *J. Phys. Chem A* **115**, 4406 (2011). 945
- [26] R. Hoffman, S. Shaik and P.C. Hiberty, *Acc. Chem. Res.* **36**, 750 (2003).
- [27] H.B. Schlegel, *Adv. Chem. Phys.* **67**, 249 (1987).
- [28] K. Fukui, *Acc. Chem. Res.* **14**, 363 (1981).
- [29] S. Shaik, A. Ioffe, A.C. Reddy and A. Pross, *J. Am. Chem. Soc.* **116**, 262 (1994). 950
- [30] H. Eyring, *J. Chem. Phys.* **3**, 107 (1935); E. Wigner, *Trans. Faraday Soc.* **34**, 29 (1938).
- [31] G.S. Hammond, *J. Am. Chem. Soc.* **77**, 334 (1955); J.E. Leffler, *Science* **117**, 340 (1953). 955
- [32] Z. Shi and R.J. Boyd, *J. Am. Chem. Soc.* **113**, 1072 (1991).
- [33] R.F.W. Bader and P.J. MacDougall, *J. Am. Chem. Soc.* **107**, 6788 (1985); N. Balakrishnan and N. Sathyamurthy, *Chem. Phys. Lett.* **164**, 267 (1989); M. Ho, H.L. Schmider and D.F. Weaver, *J. Chem. Theory Comput.* **6**, 153 (2010); V.H. Smith, Jr, R.P. Sagar and R.O. Esquivel, *Int. J. Quantum Chem.* **77**, 376 (2000); E.H. Knoerr and M.E. Eberhart, *J. Phys. Chem. A* **105**, 880 (2001); A. Tachibana, *J. Chem. Phys.* **115**, 3497 (2001). 960
- [34] S.R. Gadre, in *Reviews of Modern Quantum Chemistry: A Celebration of the Contributions of Robert G. Parr*, edited by K.D. Sen (World Scientific, Singapore, 2003); Vol. 1, pp. 108–147; T. Koga and M.J. Morita, *Chem. Phys.* **79**, 1933 (1983); S.K. Ghosh, M. Berkowitz and R.G. Parr, *Proc. Natl. Acad. Sci. USA* **81**, 8028 (1984); J.C. Angulo and J.S. Dehesa, *J. Chem. Phys.* **97**, 6485 (1992); S.E. Massen and C.P. Panos, *Phys. Lett. A* **246**, 530 (1998); R.F. Nalewajski and R.G. Parr, *J. Phys. Chem. A* **105**, 7391 (2001); A. Nagy, *J. Chem. Phys.* **119**, 9401 (2003); E. Romera and J.S. Dehesa, *J. Chem. Phys.* **120**, 8906 (2004); P. Karafiloglou and C.P. Panos, *Chem. Phys. Lett.* **389**, 400 (2004); K.D. Sen, *J. Chem. Phys.* **123**, 074110 (2005); R.G. Parr, R.F. Nalewajski and P.W. Ayers, *J. Phys. Chem. A* **109**, 3957 (2005); N.L. Guevara, R.P. Sagar and R.O. Esquivel, *J. Chem. Phys.* **122**, 084101 (2005); Q. Shi and S. Kais, *J. Chem. Phys.* **309**, 127 (2005); K.Ch. Chatzisavvas, Ch.C. Moustakidis and C.P. Panos, *J. Chem. Phys.* **123**, 174111 (2005); K.D. Sen and J. Katriel, *J. Chem. Phys.* **125**, 074117 (2006); A. Nagy, *Chem. Phys. Lett.* **425**, 154 (2006); P.W. Ayers, *Theor. Chem. Acc.* **115**, 253 (2006); L.M. Martyusheva and V.D. Seleznev, *Phys. Rep.* **426**, 1 (2006); S. Liu, *J. Chem. Phys.* **126**, 191107 (2007); A. Borgoo, P. Jaque, A. Toro-Labbé, Ch. Van Alsenoy and P. Geerlings, *Phys. Chem. Chem. Phys.* **11**, 476 (2009); P. Geerlings and A. Borgoo, *Phys. Chem. Chem. Phys.* **13**, 911 (2011). 995
- [35] R.O. Esquivel, N. Flores-Gallegos, C. Iuga, E. Carrera, J.C. Angulo and J. Antolin, *Theor. Chem. Acc.* **124**, 445 (2009).
- [36] R.O. Esquivel, N. Flores-Gallegos, C. Iuga, E. Carrera, J.C. Angulo and J. Antolin, *Phys. Lett. A* **374**, 948 (2010). 1000
- [37] S. López-Rosa, R.O. Esquivel, J.C. Angulo, J. Antolin, J.S. Dehesa and N. Flores-Gallegos, *J. Chem. Theory Comput.* **6**, 145 (2010).
- [38] D.C. Rawlings and E.R. Davidson, *J. Phys. Chem.* **89**, 969 (1985). 1005
- [39] P. Kaijser and V.H. Smith Jr, *Adv. Quant. Chem.* **10**, 37 (1997).
- [40] M. Kohout, Program *DGRID*, version 4.2, 2007.
- [41] S. López-Rosa, J.C. Angulo and J. Antolin, *Physica A* **388**, 2081 (2009). 1010
- [42] A. Dembo, T.M. Cover and J.A. Thomas, *IEEE Trans. Inform. Theory* **37**, 1501 (1991).
- [43] M.J. Frisch, G.W. Trucks, H.B. Schlegel, G.E. Scuseria, M.A. Robb, J.R. Cheeseman, J.A. Montgomery, Jr, T. Vreven, K.N. Kudin, J.C. Burant, J.M. Millam, S.S. Iyengar, J. Tomasi, V. Barone, B. Mennucci, M. Cossi, G. Scalmani, N. Rega, G.A. Petersson, H. Nakatsuji, M. Hada, M. Ehara, K. Toyota, R. Fukuda, J. Hasegawa, M. Ishida, T. Nakajima, Y. Honda, O. Kitao, H. Nakai, M. Klene, X. Li, J.E. Knox, H.P. Hratchian, J.B. Cross, V. Bakken, C. Adamo, J. Jaramillo, R. Gomperts, R.E. Stratmann, O. Yazyev, A.J. Austin, R. Cammi, C. Pomelli, J.W. Ochterski, P.Y. Ayala, K. Morokuma, G.A. Voth, P. Salvador, J.J. Dannenberg, V.G. Zakrzewski, S. Dapprich, A.D. Daniels, M.C. Strain, O. Farkas, D.K. Malick, A.D. Rabuck, K. Raghavachari, J.B. Foresman, J.V. Ortiz, Q. Cui, A.G. Baboul, S. Clifford, J. Cioslowski, B.B. Stefanov, G. Liu, A. Liashenko, P. Piskorz, I. Komaromi, R.L. Martin, D.J. Fox, T. Keith, M.A. Al-Laham, C.Y. Peng, A. Nanayakkara, M. Challacombe, P.M.W. Gill, B. Johnson, W. Chen, M.W. Wong, C. Gonzalez and J.A. Pople, *Gaussian 03, Revision D.01* (Gaussian, Inc., Wallingford, CT, 2004). 1015
- [44] B.A. Johnson, C.A. Gonzales, P.M.W. Gill and J.A. Pople, *Chem. Phys. Lett.* **221**, 100 (1994).
- [45] J.M. Pérez-Jordá and E. San-Fabián, *Comput. Phys. Commun.* **77**, 46 (1993); J.M. Pérez-Jordá, A.D. Becke and E. San-Fabián, *J. Chem. Phys.* **100**, 6520 (1994). 1040